1   **DNA Release from Complex Plant Tissue using Focused Ultrasound Extraction (FUSE)**

2

3   Alexia Stettinius[1], Hal Holmes[1,2], Qian Zhang[3], Isabelle Mehochko[1], Misa Winters[2], Ruby Hutchison[1], Adam

4   Maxwell[4], Jason Holliday[3], Eli Vlaisavljevich[1]

5

6   [1]Department of Biomedical Engineering and Mechanics, Virginia Polytechnic Institute and State
7   University, Blacksburg, VA, USA
8   [2]Conservation X Labs, Seattle, WA, USA
9   [3]Department of Forest Resources and Environmental Conservation, Virginia Polytechnic Institute and
10   State University, Blacksburg, VA, USA
11   [4]Department of Urology, University of Washington, Seattle, WA, USA
12

13   **Abstract:**

14   Sample preparation in genomics is a critical step that is often overlooked in molecular

15   workflows and impacts the success of downstream genetic applications. This study explores the

16   use of a recently developed focused ultrasound extraction (FUSE) technique to enable the rapid

17   release of DNA from plant tissues for genetic analysis. FUSE generates a dense acoustic

18   cavitation bubble cloud that pulverizes targeted tissue into acellular debris. This technique was

19   applied to leaf samples of American chestnut (*Castanea dentata*), tulip poplar (*Liriodendron*

20   *tulipifera*), red maple (*Acer rubrum*), and chestnut oak (*Quercus montana*). We observed that

21   FUSE can extract high quantities of DNA in 9-15 minutes, compared to the 30 minutes required

22   for conventional DNA extraction. FUSE extracted DNA quantities of 24.33 ± 6.51 ng/mg and

23   35.32 ± 9.21 ng/mg from American chestnut and red maple, respectively, while conventional

24   methods yielded 6.22 ± 0.87 ng/mg and 11.51 ± 1.95 ng/mg, respectively. The quality of the

25   DNA released by FUSE allowed for successful amplification and next-generation sequencing.

26   These results indicate that FUSE can improve DNA extraction efficiency for leaf tissues.

1

27   Continued development of this technology aims to adapt to field-deployable systems to

28   increase the cataloging of genetic biodiversity, particularly in low-resource biodiversity

29   hotspots.

1. Introduction

Over the past two decades, developments in genome sequencing technologies have enabled researchers to provide an unprecedented scope and depth of genetic information. Emerging technologies have equipped researchers with the tools to perform DNA and RNA sequencing in the field [1], which could allow for new genetics research to be carried out by non-scientists in a variety of settings that had not previously been feasible [2-4]. Despite technological advancements, novel sequencing platforms cannot be applied to all sample types, including many plant species, due to the poor representation of plant genomes in genetic databases. For example, of the nearly 400,000 unique plant species estimated to exist, only 600 have nearly complete genome coverage and assembly [5]. A recent review surveying commonly referenced databases found that only 17.7% of plants had broad genetic coverage, 80% of plant species had limited data availability, and some had no information other than their taxonomic names reported [6]. With such little coverage of plant taxa, it is likely that many opportunities for new uses of undiscovered traits unique to species have gone unnoticed, and with extinction rates rising, we may lose some of these opportunities forever. Sequencing plant genomes is also essential for utilizing genetic resources in breeding programs [7], conserving plant species [8, 9], understanding their role in ecosystem function [6, 10, 11], and phylogenetic studies [12]. Therefore, continued expansion of plant genetic databases is essential to spur discovery, drive innovation, and protect crucial resources. To accomplish this, tools for more efficient DNA extraction are necessary. Despite recent advancements in genome sequencing, DNA extraction technologies have lagged behind, particularly for complex plant tissues where the cell walls and membranes need to be broken down without significantly degrading the genetic material.

3

52   Therefore, sample preparation and DNA extraction remain a painful barrier that prevents rapid

53   and inexpensive sequencing of plant genomes.

54

55   All genetic testing platforms require the input of purified genetic material. Consequently, a

56   robust DNA extraction protocol that yields DNA of sufficient concentration and purity is essential

57   for success in subsequent genotyping and sequencing applications. In plants, the release of viable

58   DNA is hindered by tough tissue matrices that are resistant to mechanical breakdown, the

59   presence of polysaccharide-rich cell walls, and many inhibitory compounds such as polyphenolic

60   metabolites [4, 13, 14]. To combat these challenges, manual tissue pulverization with benchtop

61   tools, such as a mixer mill, or a mortar and pestle under liquid nitrogen, is used in conjunction

62   with plant cell lysis and purification protocols. Plant DNA extraction is often cumbersome, and

63   despite specialized tissue breakdown strategies, releasing DNA suitable for genomic analysis is

64   challenging for many sample types. Additionally, current DNA extraction techniques require an

65   advanced laboratory [15, 16]. With the rise of point-of-contact genetic testing, the ability to

66   translate DNA extraction protocols to the field is becoming increasingly important [3, 17]. For

67   plants, the simplification of DNA extraction could be pivotal in conservation efforts where

68   researchers must rapidly and inexpensively prepare samples from biodiversity hotspots, which

69   are often remote and far removed from centralized laboratories [3, 18, 19].

70

71   Our group has recently developed a new technology capable of accelerating and simplifying the

72   DNA extraction workflow, termed focused ultrasound extraction (FUSE), to address sample

73   preparation and DNA extraction challenges. FUSE has previously demonstrated its capacity to

74   rapidly release DNA from Atlantic salmon muscle tissue samples with intense cavitation clouds

75   generated by focused ultrasonic transducers [20]. This technology employs dense acoustic

76   cavitation bubble clouds similar to those used in histotripsy, a non-invasive focused ultrasound

77   therapy currently being developed for medical applications [21, 22]. During FUSE, the rapid

78   expansion and violent collapse of the cavitation microbubbles induce high stress on the target

79   tissue, which causes mechanical disintegration and results in an acellular tissue lysate [23, 24].

80   The tissue lysate is then collected, and the released DNA is purified for downstream analyses.

81   This process differs from conventional extraction methods that require samples to be pulverized

82   by hand using a mortar and pestle or automated homogenizer under liquid nitrogen and require

83   elongated incubation periods varying from 10 minutes to 1 hour, depending on the plant tissue,

84   before DNA collection and purification (Figure 1).
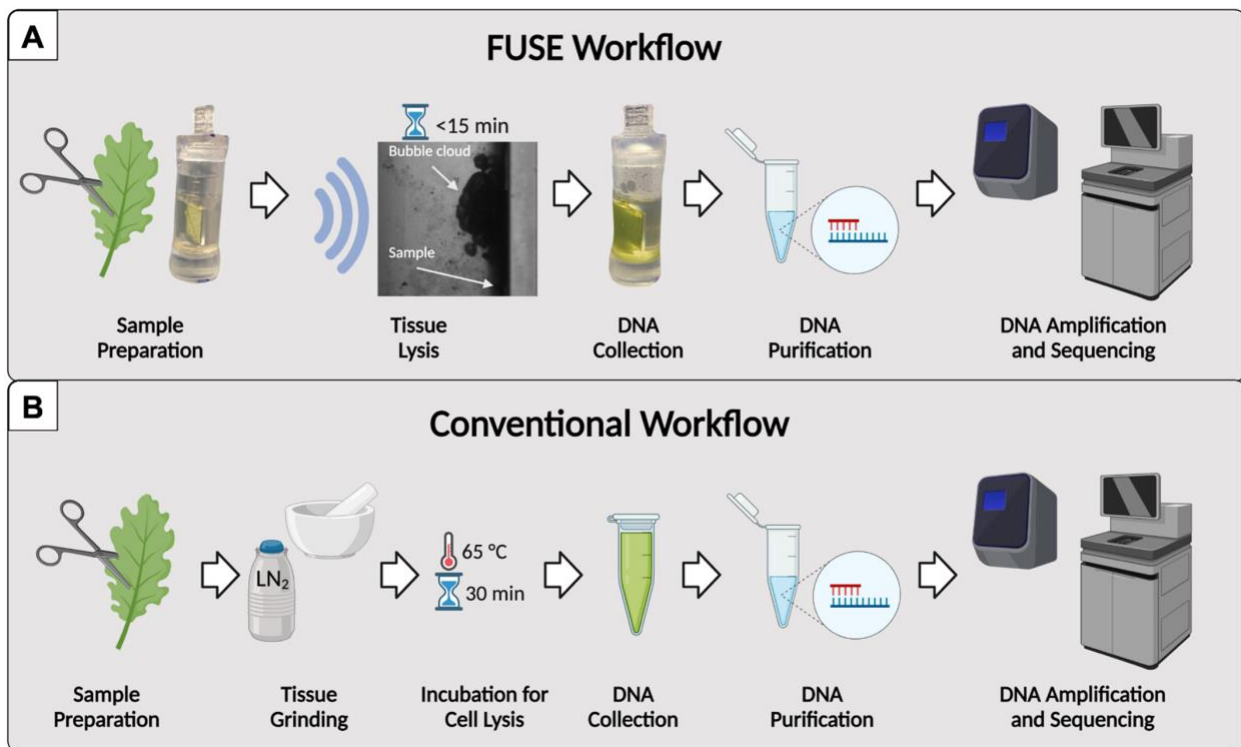
85

86   *Figure* 1*: DNA extraction workflow. The process begins with sample preparation for FUSE and conventional DNA*

87   *extraction protocols. In both cases, leaf samples are trimmed and massed before tissue processing. For FUSE, the*

88   *prepared sample is aligned with the cavitation bubble cloud, and the tissue is sonicated in 15 minutes or less,*

89   *eliminating the need for incubation. In both protocols, the DNA is then collected and purified. In the conventional*

90   *extraction protocol, tissue processing involves manual grinding under liquid nitrogen and a 30-minute minimum*

91   *incubation period. Following purification, the samples are prepared for amplification and sequencing.*

92   Here, we test the efficacy of FUSE with plant tissue by 1) determining the feasibility of leaf tissue

93   breakdown, 2) measuring the DNA yield, 3) amplifying the released DNA with PCR to verify DNA

94   quality, and 4) sequencing the resultant DNA libraries to validate the utility of FUSE in whole-

95   genome sequencing applications. While our ultimate goal is to adapt FUSE to low-cost and field-

96   deployable systems to enable rapid sample processing and DNA extraction from various sample

97   types, here we address the feasibility of FUSE for DNA release from leaf tissue in a laboratory

98   setting using prototype transducers and custom acoustically transparent sample holders. We

99   hypothesize that FUSE can pulverize leaf tissue and yield significant quantities of DNA with a

100   quality suitable for PCR amplification and next-generation sequencing. If successful, FUSE could

101   streamline plant DNA extraction workflows to improve standard laboratory practices. Further

102   technology development could allow the miniaturization of the FUSE system to bring this

103   technology to the field to expand the scope of opportunities.

104

105   **2. Materials and Methods**

106   To demonstrate the ability of FUSE to rapidly provide amplifiable DNA fragments for genetic

107   analysis, we used frozen leaf samples collected from American chestnut (*C. dentata*), tulip poplar

108   (*L. tulipifera*), red maple (*A. rubrum*), and chestnut oak (*Q. montana*) trees that were stored at -

109   20 °C before use. These species were selected because they were locally available and

110   represented a wide range of angiosperm taxonomic diversity that may correspond to variation in

111   physical properties and secondary metabolite composition. The tissue samples were prepared

112   and processed under the following experimental conditions:

113

114   2.1. FUSE Pulse Generation

115   A custom 32-element 500 kHz array transducer with a geometric focus of 75 mm, an aperture

116   size of 150 mm, and an effective f-number of 0.58 was used for all experiments in this study

117   [25]. A custom high-voltage pulser was used to drive the transducer and generate a short single

118   cycle ultrasound pulse. The pulser was connected to a field-programmable gate array (FPGA)

119   board (Altera DE0-Nano Terasic Technology, Dover, DE, USA), which was explicitly programmed

120   for histotripsy therapy pulsing. A custom-built fiber-optic probe hydrophone (FOPH) [26] was

121   used to measure the acoustic output pressure of the transducers. The FOPH was cross-

122   calibrated at low-pressure values using a reference hydrophone (Onda HNR-0500) to ensure

123   accurate pressures were measured from the FOPH. The lateral and axial full width half

124   maximum (FWHM) dimensions at the geometric focus of the transducer were measured to be

125   2.3 mm and 7.1 mm, respectively. The acoustic pressures used for all experiments were

126   measured in degassed water at the focal point of the transducer, which was identified using a

127   3D beam scan. The acoustic output could not be directly measured at higher pressure levels (p-

128   > 16 MPa) due to cavitation at the fiber tip. These pressures were estimated by summating the

129   output focal p- values from individual transducer elements. For all samples in this study, a

130   pressure of ~34 MPa was applied for FUSE processing.

7

131

2.2. Visualization of FUSE Tissue Disintegration

For all focused ultrasound experiments, high-speed optical imaging was done using a machine-vision camera (Blackfly S 3.2MP Mono USB3 Vision, FLIR Integrated Imaging Solutions, Richmond, BC, Canada) that was aligned with the focal zone of the transducer using a 100 mm F2.8 Macro lens (Tokina AT-X Pro, Kenko Tokina Co., LTD, Tokyo, Japan) and backlit by a custom-built pulsed LED strobe light capable of high-speed triggering with 1 μs exposures. As done in previous studies, the camera and the strobe light were triggered individually by the amplifier box, with the camera shutter opening at the time of pulse generation and the strobe acting as the shutter [27, 28]. The camera was triggered to capture one image every 50th pulse. The exposures were centered at delay times of 6, 48.5, and 98.5 μs after the pulse arrived at the focus to allow visualization of bubble cloud formation, coalescence, and collapse.

2.3. Sample Preparation

Three leaves of American chestnut, tulip poplar, red maple, and chestnut oak were processed with FUSE and conventional extraction methods. Half of each leaf was used for FUSE, and the other half was used for conventional extraction (Figure S1). Three samples were acquired from each half. All samples processed with FUSE were prepared as 12 mm squares using a sterile scalpel blade. The mass of FUSE samples ranged from 10-30 mg, depending on the thickness of the sample.

2.3.i. FUSE Experimental Configuration

8

153   Leaf tissue samples were secured in a custom-designed sample holder positioned in the axial

154   focus of the transducer, located between the camera and light source. The sample holder was

155   designed to support a 12.5 mm x 12.5 mm x 1 mm sapphire glass window, the sample, and a

156   polyethylene terephthalate glycol (PETG) square frame that secured the sample on the surface

157   of the glass backing. The assembled sample holder was placed inside an optically transparent

158   and acoustically permeable tube with an inner diameter of 9.525 mm and a wall thickness of

159   1.59 mm (Tygon PVC E-1000, McMaster-Carr, Douglasville, GA, USA). When the sample holder

160   was placed in the tube, cylindrical appendages at the top and bottom of the sample holder

161   created a controlled volume chamber for the DNA lysis buffer. The upper appendage featured

162   a small circular opening for applying the DNA lysis buffer. A custom-built mount suspended the

163   tube assembly in the water tank for tissue processing, and a stopper was designed to seal the

164   other end of the tube. A robotic positioning system controlled by custom MATLAB scripts was

165   used to align samples with the focus of the ultrasonic transducer (Figure 2).

9
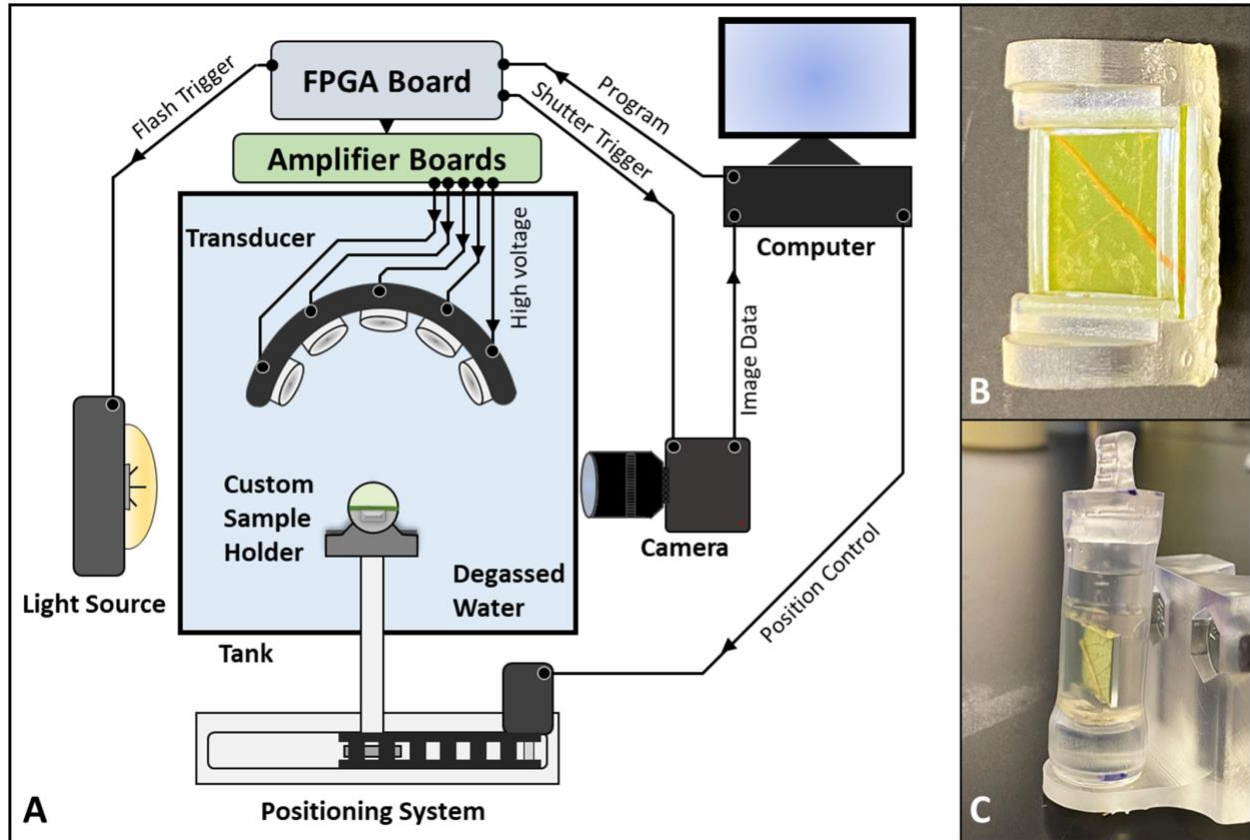
Figure 2: Experimental FUSE set-up. (A) Ultrasonic transducers are driven by an FPGA board and amplifier. High-speed imaging is performed using a strobe and camera controlled by signals from the FPGA board. Custom scripts are delivered to the FPGA board, and imaging data is recorded by a computer. A robotic positioning system, controlled by the computer using MATLAB, is used to align the sample in the focus of the transducer array. (B) A custom sample holder designed to support a sapphire glass backing, the leaf sample, and a PETG frame is used. (C) The sample holder assembly is housed in an acoustically permeable tube for DNA extraction experiments.

The configuration of the sample and sapphire glass backing in the focus of the transducer was chosen to maximize the efficiency of tissue sonication with FUSE. When ultrasonic pulses generate a cavitation bubble cloud near a rigid boundary, high-pressure collapse is expected to occur toward the surface of the boundary [29-31]. Figure 3 demonstrates this effect. As the time after pulse arrival increased, microbubble coalescence became more evident, and the

178   concentration of bubbles near the sample surface increased. Sapphire glass was chosen because

179   it is hydrodynamically strong and has a high acoustic impedance. The hydrodynamic strength of

180   the sapphire glass provided an unyielding surface to support the sample when exposed to high-

181   pressure fluid flow caused by cavitation. The high acoustic impedance increased the pressure

182   near the boundary and induced the cavitation bubbles to grow larger and collapse more violently.

183   Overall, this effect maximized the impact pressure felt by the sample. In preliminary experiments,

184   FUSE was tested without including the sapphire glass backing and sample holder. With this

185   configuration, the sample was free to move outside of the focal zone, which decreased the tissue

186   disintegration efficiency of FUSE and caused inconsistencies in tissue breakdown success.
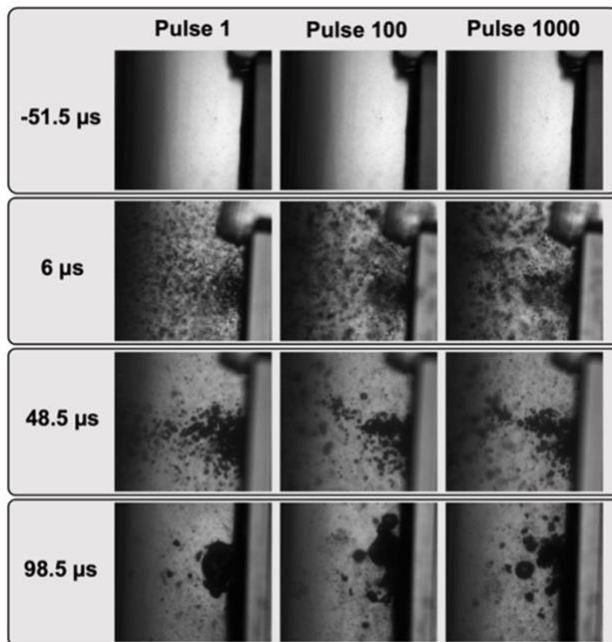
187

188   *Figure 3:* *The cavitation bubble cloud collapses toward the surface of the leaf tissue. 51.5 μs before pulse arrival (row*

189   *1), the sample and sapphire glass backing are imaged. 6 μs after pulse arrival (row 2), the cavitation cloud is visible*

190   *and contains many microbubbles that have not substantially expanded or coalesced. As time progresses (rows 3), the*

191   *microbubbles begin to coalesce and are concentrated near the sample's surface. 98.5 μs after pulse arrival (row 4),*

192   *the microbubbles are near collapse and situated adjacent to the sample.*

193

194 *2.3.ii. Control Sample Preparation and Tissue Lysis*

195 Control samples were obtained by cutting the leaf tissue into 100 mg segments, and samples

196 were disrupted by grinding with mortar and pestle under liquid nitrogen. 100 mg control samples

197 were put in the mortar; liquid nitrogen was added to freeze the samples and cool the mortar,

198 pestle, and spatula. To begin, grinding with the pestle was done slowly, and once the liquid

199 nitrogen was mostly evaporated, more vigorous grinding was performed to reduce the tissue to

200 a fine powder. The tissue powder was then transferred to a 1.5 mL centrifuge tube where 400 µL

201 of 1% PVP-40 Buffer AP1 solution and 4 µL of RNase A were added (Qiagen DNeasy Plant Kit

202 Qiagen Inc, Hilden, Germany). The tube was initially vortexed to homogenize the solution before

203 incubation at 65 °C for 30 minutes with a short vortex every 5 minutes.

204

205 2.4 FUSE Tissue Disintegration

206 Leaf tissue samples were processed using single cycle ultrasound pulses delivered at a pressure

207 of 34 MPa and a pulse repetition frequency (PRF) of 500 Hz. Measurements made with a fiber

208 optic hydrophone determined that pressure loss was negligible (<1%) when pulses were

209 delivered through the sample tube. Before tissue processing, the acoustic focus was directed at

210 the center of the sample. To completely disintegrate the leaf tissue sample, MATLAB scripts

211 controlling the positioning system were designed to move the sample in a spiral square pattern

212 such that each point within the 100 mm^2 disintegration zone was exposed to the focal bubble

213 cloud for 0.5 s. Using this approach, a single scan of the applied pattern delivered 250 pulses per

214 point, with multiple scans used for each sample to achieve sufficient tissue breakdown. To

215 account for potential differences in the physical properties of the selected leaf species, the

216 number of scans required for complete tissue disintegration was initially characterized for

217 American chestnut, tulip poplar, red maple, and chestnut oak samples (n=3) backed with

218 sapphire glass suspended in an open water bath. Images of the sample were taken after each

219 scan. Each image was converted to grayscale, then to binary using the Otsu method [32]. The

220 targeted tissue area was mapped as an ROI with dimensions of 10 x 10 mm to represent the area

221 exposed to ultrasonic pulses. The disrupted tissue area inside and outside the ROI was quantified

222 by counting the number of pixels using custom MATLAB scripts. Pixel counts were converted to

223 tissue disintegration area. The significance of the area measurements was determined using an

224 unpaired student's t-test with unequal variance. Values less than 0.05 ($p < 0.05$) were considered

225 significant.

226

227 2.5 Purification Conditions

228 The robustness of the DNA extraction process was investigated through purification of the

229 disintegrated tissue and quantification of the released DNA. DNA was extracted from samples of

230 American chestnut, tulip poplar, red maple, and chestnut oak with FUSE (n = 9) and conventional

231 extraction methods (n = 9) using a lysis buffer and purified using silica columns (Qiagen DNeasy

232 Plant Kit Qiagen Inc, Hilden, Germany). All lysates were analyzed with a Qubit™ 4 Fluorometer

233 (ThermoFisher, Waltham, MA, USA) and a Nanodrop™ One (ThermoFisher, Waltham, MA, USA)

234 to determine the quantity and quality of DNA released with FUSE and control samples. DNA yield

235 was reported as the quantity of DNA released per milligram of tissue to normalize input sample

236   mass. For data acquired from Nanodrop™ and Qubit™ measurements, an unpaired student's t-

237   test with unequal variance was used, with values less than 0.05 ($p<0.05$) considered significant.

238

239   FUSE and control samples were purified with a lysis buffer containing 1% PVP-40 Buffer AP1

240   solution and RNase A. The lysis buffer used on the FUSE samples consisted of 1 mL of 1% PVP-40

241   Buffer AP1 solution and 8 µL of RNase A (0.8 mg), and samples were soaked for the duration of

242   FUSE tissue sonication. The lysis buffer volume used for the controls varied depending on the

243   quality of the leaf tissue sample, which was determined based on the color and age assessment.

244   For older samples with a dark green or brown-green color, 1 mL of 1% PVP-40 Buffer AP1 solution

245   and 8 µL of RNase A (0.8 mg) were used. For younger samples with a yellow-green color, 500 µL

246   of 1% PVP-40 Buffer AP1 solution and 4 µL of RNase A (0.4 mg) were used. This was done because

247   the leaves with a lower water content yielded a larger sample volume after grinding with mortar

248   and pestle under liquid nitrogen and therefore required a greater buffer volume for proper cell

249   lysis. Subsequent purification of FUSE and control samples was performed in silica columns using

250   the standard protocol as recommended by the manufacturer (Qiagen DNeasy Plant Kit Qiagen

251   Inc, Hilden, Germany).

252

253   2.6 PCR Amplification

254   To compare the two methods for downstream genotyping, American chestnut genomic DNA

255   extracted by FUSE and conventional methods was subjected to a genotyping by sequencing (GBS)

256   workflow that involved restriction digestion followed by ligation of sequencing adapters and PCR

257   amplification [33]. American chestnut samples processed with FUSE and conventional methods

258 were normalized to 55 ng, then digested with 1 μL of ApeKI (New England BioLabs, Ipswitch, MA,

259 USA). This restriction enzyme recognizes a 5 bp degenerate sequence GCWGC, where W is an A

260 or T [34]. For one of the American chestnut samples processed with FUSE, the quantity of eluted

261 DNA did not reach 55 ng, so 36.2 ng of DNA was used in the digestion reaction. The resulting DNA

262 fragments were ligated to Illumina-compatible adapters with 1.6 μL of T4 DNA ligase. P1 adapters

263 contained a unique barcode region for each adapter immediately upstream of the ligated DNA

264 fragment, and the P2 adapter was consistent for all samples. PCR was performed under the

265 following conditions: 95 °C for 1 minute, followed by 18 cycles of 95 °C for 30 seconds, 63 °C for

266 20 seconds, and 68 °C for 30 seconds. Lastly, samples were brought to 68 °C for 5 minutes and

267 kept at 4 °C. PCR primers contained complementary sequences for amplifying restriction

268 fragments with ligated adapters [34]. Ligation and amplification were assessed by gel

269 electrophoresis for all samples. Six samples, three processed with FUSE and three processed with

270 conventional methods, were viewed using a 2100 Bioanalyzer instrument (2100 Bioanalyzer,

271 Agilent, Santa Clara, CA, USA) to compare the fragment size distribution for individual PCR

272 products yielded by FUSE and conventional methods. DNA samples were purified before and

273 after PCR with the Monarch® PCR and DNA Clean-Up Kit (New England Biolabs, Ipswitch, MA,

274 USA). Individual sample libraries were pooled, and fragments ranging from 250-550 bp were

275 selected using BluePippin™ (Sage Science, Beverly, MA, USA). The resulting library was visualized

276 using a 2100 Bioanalyzer instrument.

277

278 2.7 Sequencing Analysis

15

279   The American chestnut GBS libraries were sequenced with the NovaSeq 6000 instrument

280   (Illumina, San Diego, CA, USA) in 2x150 bp paired-end mode at Duke University Center for

281   Genomic and Computational Biology. Raw reads were filtered for quality and adapter

282   contamination, then demultiplexed using STACKS software [35]. Filtered reads were aligned to

283   v.1.1 of the *C. dentata* reference genome [36] using the Burrows-Wheeler Aligner (BWA) mem

284   algorithm and subsequently converted to BAM format with SAMtools [33]. Heterozygous sites

285   were called with the Genome Analysis Toolkit (GATK) HaplotypeCaller algorithm [37, 38], and

286   these GVCFs were then merged using the GenotypeGVCFs function. Variants were flagged and

287   removed as low quality if they had the following characteristics: low map quality ($MQ < 40$); high

288   strand bias ($FS > 40$); differential map quality between reads supporting the reference and

289   alternative alleles ($MQRankSum < -12.5$); bias between the reference and alternate alleles in the

290   position of alleles within the reads ($ReadPosRankSum < -8.0$); and low depth of coverage ($DP <$

291   5). Coverage depth per sample was calculated using the SAMtools depth function. Statistical

292   analysis of coverage depth was performed using a Wilcoxon rank-sum test with values less than

293   0.05 ($p<0.05$) considered significant.

294

295   **3. Results & Discussion**

296   3.1 FUSE Tissue Disintegration

297   The feasibility of FUSE for leaf tissue disintegration was examined with American chestnut, tulip

298   poplar, red maple, and chestnut oak leaves by characterizing tissue breakdown after each FUSE

299   scan. Images were captured after each scan to demonstrate the progression of tissue

300   disintegration for each species (Figure 4). In all cases, the damaged tissue area increased with

16

301   increasing scan number, but the number of scans required to achieve significant tissue

302   breakdown differed among species. Tulip poplar leaves were the most vulnerable to breakdown,

303   as they were the only species with notable tissue disintegration after one scan. The extent of

304   tulip poplar tissue disruption increased with each scan. For the American chestnut and red maple

305   samples, scans one and two generated minimal tissue breakdown, but after scan three, the area

306   of tissue breakdown was more observable. For American chestnut, the tissue in the targeted

307   region was completely disrupted after four scans. For red maple, the tissue breakdown continued

308   to increase after scans four, five, and six. For American chestnut, tulip poplar, and red maple

309   samples, tissue breakdown beyond the bounds of the targeted disintegration zone was observed.

310   This effect was likely due to dispersed cavitation occurring outside the focal point of the

311   converging pressure fronts. Surface inhomogeneities at solid-liquid interfaces result in the

312   growth of cavitation nuclei that can induce cavitation at thresholds below the intrinsic threshold

313   [39, 40]. Previous work has also shown that leaves are more susceptible to cavitation-induced

314   tissue disruption when gas channels are present in the tissue [41, 42]. Therefore, it is possible

315   that the surface architecture and distribution of gas channels within the tissue matrices created

316   cavitation nucleation sites outside the targeted area. It is also possible that residual gas bubbles

317   from preceding pulses diffused outside the focus and served as cavitation nuclei. This would

318   induce cavitation below the intrinsic pressure threshold and expose a larger area of the leaves to

319   cavitation [43]. Lastly, off-target leaf tissue disintegration could result from acoustic shielding,

320   such that the residual bubbles in the acoustic focus increased the likelihood of acoustic scattering

321   [44, 45]. The trends in tissue breakdown for chestnut oak differed from the other three species.

322   Visible tissue breakdown was not observed until after the third scan, and tissue disintegration in

17

323   the following scans did not progress as promptly as it did for the American chestnut, tulip poplar,

324   and red maple samples. It is expected that variation in tissue breakdown across species was due

325   to differences in physical properties, such as the water content and tissue strength.

326
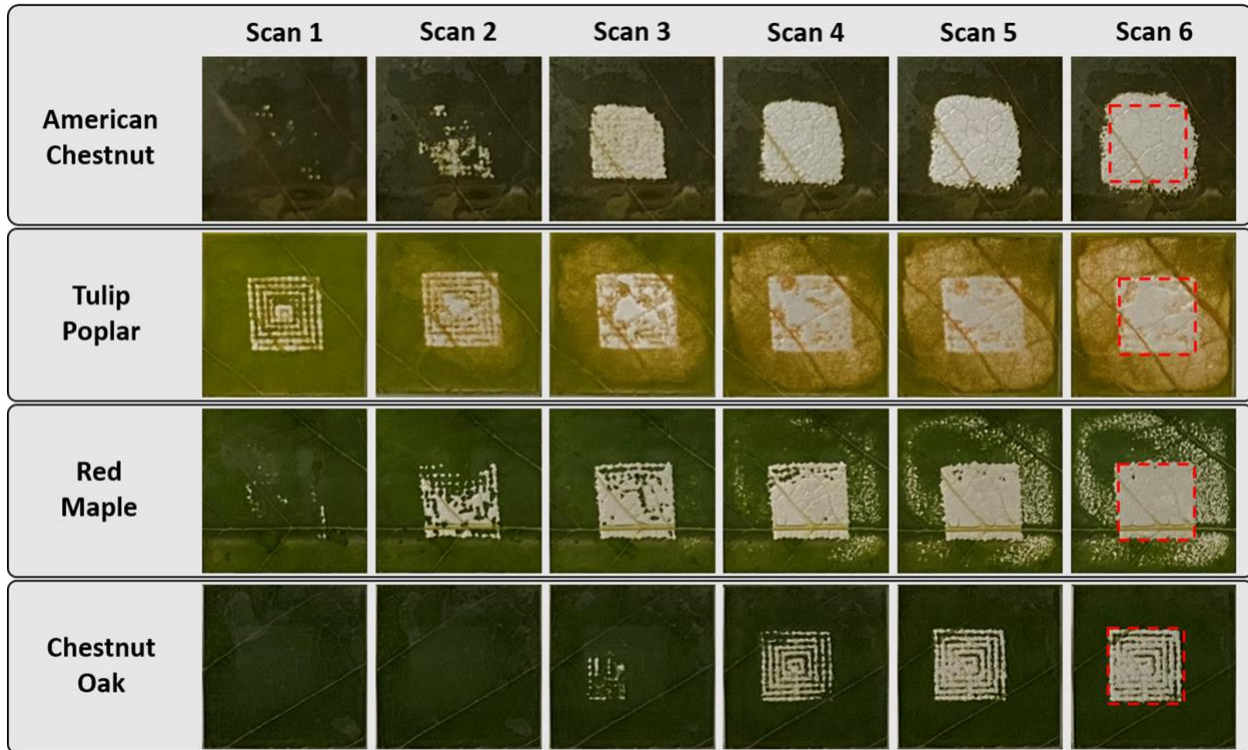
Figure 4: Leaf tissue disintegration increases after each FUSE scan. The red square in the top right identifies the targeted tissue region. Tissue breakdown beyond the target area is the result of peripheral cavitation damage. Image data suggests that the leaf species affect FUSE tissue disintegration efficiency.

330   The observed efficiency of FUSE tissue disintegration was assessed quantitatively by plotting the

331   disintegration area inside the targeted region and the total disintegration area as a function of

332   scan number for American chestnut, tulip poplar, red maple, and chestnut oak leaves (Figure 5).

333   The initial breakdown occurred the most rapidly in tulip poplar leaves, as after scan one, $38.4 \pm$

334   11.4% of the targeted tissue region was disintegrated. In comparison, <10% of target tissue was

335   disintegrated after scan one for American chestnut, red maple, and chestnut oak. The targeted

18

336   tulip poplar tissue region was significantly processed after two scans (p<0.05 compared to zero

337   scans), and >90% of the targeted area was processed after four scans. After six scans, a final

338   disintegration area of $97.4 \pm 0.34\%$ was observed within the targeted region. The initial

339   breakdown of American chestnut leaves did not occur as rapidly as tulip poplar, but American

340   chestnut quickly approached complete tissue breakdown, reaching >90% of tissue breakdown

341   inside the targeted area after three scans. American chestnut leaves were significantly processed

342   after three scans (p<0.05 compared to zero scans), and six scans resulted in a disintegration area

343   of $99.3 \pm 0.75\%$ inside the targeted region. Red maple leaves were more resistant to breakdown

344   than tulip poplar and American chestnut, as four scans were required to achieve significant

345   breakdown (p<0.05 compared to zero scans). Interestingly, the degree of breakdown for red

346   maple in the targeted region never surpassed 90%. After six scans, the final disintegration area

347   within the targeted region for red maple was 89.2 6.0%. The observed reduction in tissue

348   breakdown efficiency could be due to the presence of the midrib, the central vein of the leaf.

349   Previous work investigating the effects of ultrasonic cavitation on *Elodea* leaves found that when

350   ultrasound was targeted at the midrib, there was a lack of cell disruption [42]. Although tulip

351   poplar, American chestnut, and red maple samples achieved significant breakdown in less than

352   six scans, increasing the scan number decreased the margin of error in the disintegration area.

353   Therefore, six scans were used to process American chestnut, tulip poplar, and red maple

354   samples to allow more consistent comparisons. Six scans resulted in a 9-minute tissue processing

355   time and a total of 1,500 pulses per point. Chestnut oak was the most resistant to breakdown.

356   After scan six, only $56.0 \pm 22.9\%$ of the targeted area was processed, so up to ten scans were

357   applied to chestnut oak leaves. Chestnut oak samples required eight scans to achieve a significant

358   breakdown of $76.6 \pm 13.8\%$ (p<0.05 compared to zero scans). Since increasing the scan number

359   increased the area of disintegration and reduced the margin of error in the disintegration area,

360   ten scans were used for chestnut oak tissue processing. Ten scans resulted in a 15-minute tissue

361   processing time and 2,500 pulses per point. The final disintegration area within the targeted

362   region for chestnut oak was $83.7 \pm 10.6\%$.

363

364   Leaf tissue breakdown outside of the targeted area was also quantified to examine the effects of

365   dispersed cavitation. Trends in tissue breakdown outside of the targeted area were comparable

366   to those observed within the targeted area, such that the tissue disintegration area increased

367   with increasing scan number. Additionally, the extent of American chestnut, tulip poplar, and red

368   maple tissue disintegration outside the targeted region was greater than chestnut oak. These

369   results suggest that differences in the physical properties among leaf species also affect the

370   extent of collateral tissue breakdown. However, collateral tissue breakdown is not of central

371   importance for this study because the samples are restricted to the size of the targeted region in

372   DNA extraction experiments.
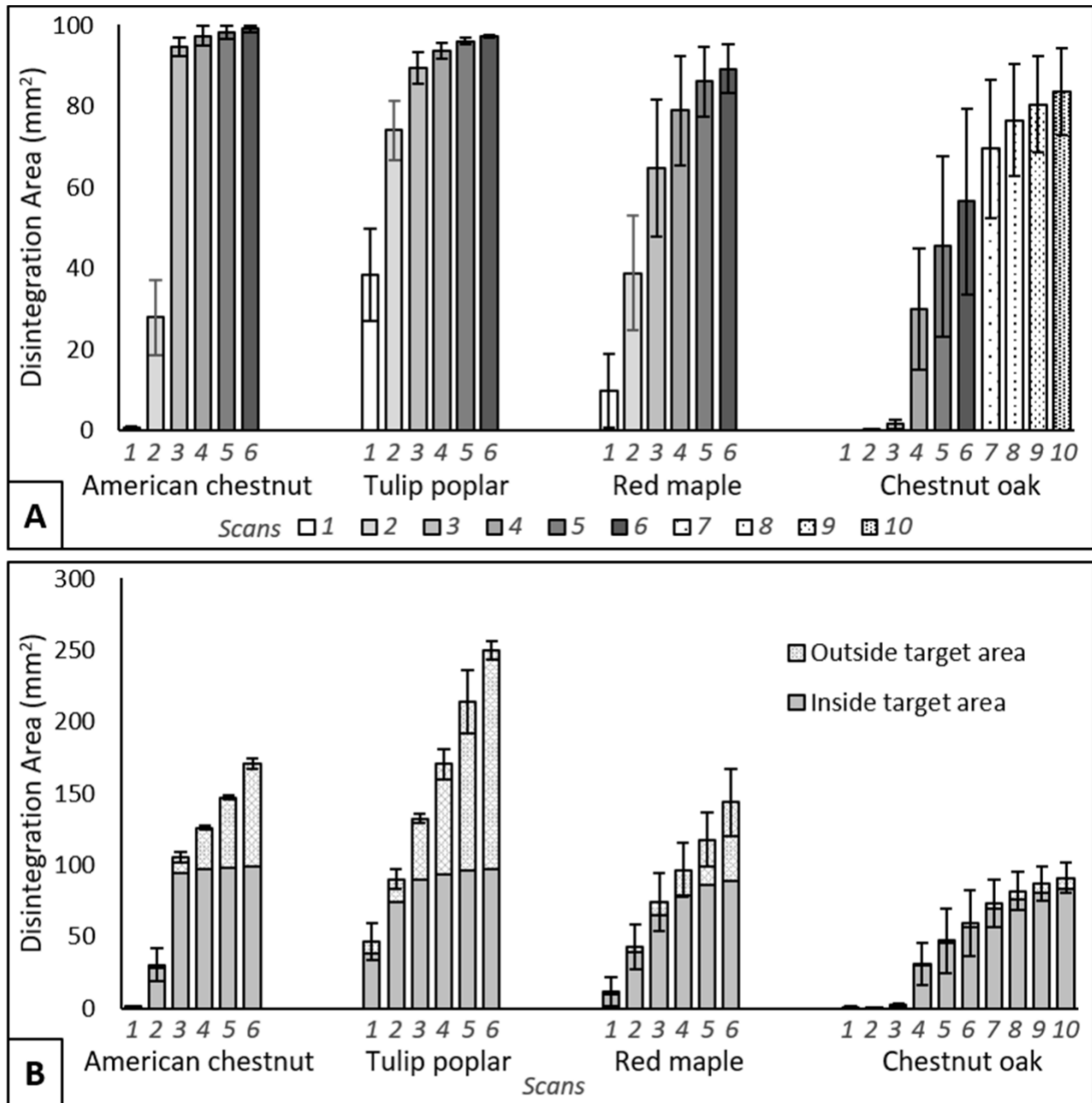
Figure 5: The leaf tissue disintegration area increases inside and outside the target area with the number of FUSE scans. (A) The disintegration area within the target area increases after each scan for all species. (B) The total disintegration area shows that tissue outside of the target area is also disintegrated by FUSE. Six scans are used for processing American chestnut, tulip poplar, and red maple samples. Chestnut oak samples required ten scans for processing due to a reduction in disintegration efficiency.

380   3.2 DNA Extraction Feasibility

381   The determined number of FUSE scans required to disintegrate each leaf species was applied to

382   the DNA extraction workflow to characterize the quantity of DNA released by FUSE compared to

383   conventional methods, the control protocol in this study (Figure 6). Overall, FUSE was able to

384   release greater quantities of DNA than conventional extraction methods in a fraction of the

385   processing time. Notably, FUSE increased the DNA yield with less than half of the input sample

386   mass required by the conventional protocol. The quantity of DNA released with FUSE and controls

387   varied with species. The DNA yield provided by six FUSE scans was significantly greater than

388   controls for American chestnut and red maple samples. Six FUSE scans released 24.3 ± 6.5 ng/mg

389   from American chestnut and 35.3 ± 9.3 ng/mg from red maple samples, while controls yielded

390   6.2 ± 0.87 ng/mg and 11.5 ± 1.9 ng/mg, respectively. No significant differences were observed in

391   the quantity of DNA released from tulip poplar samples between six FUSE scans, 32.6 ± 7.8

392   ng/mg, and controls, 28.4 ± 1.8 ng/mg. For chestnut oak leaves, 37.9 ± 5.9 ng/mg of DNA was

393   provided by ten FUSE scans, 10.7 ± 1.7 ng/mg from six FUSE scans, and 17.2 ± 2.0 ng/mg from

394   controls. The DNA yield provided by ten FUSE scans was significantly greater than six FUSE scans

395   and controls for chestnut oak samples, showing that the capacity of FUSE to release DNA from

396   tough tissues improves with an increased number of processing scans.
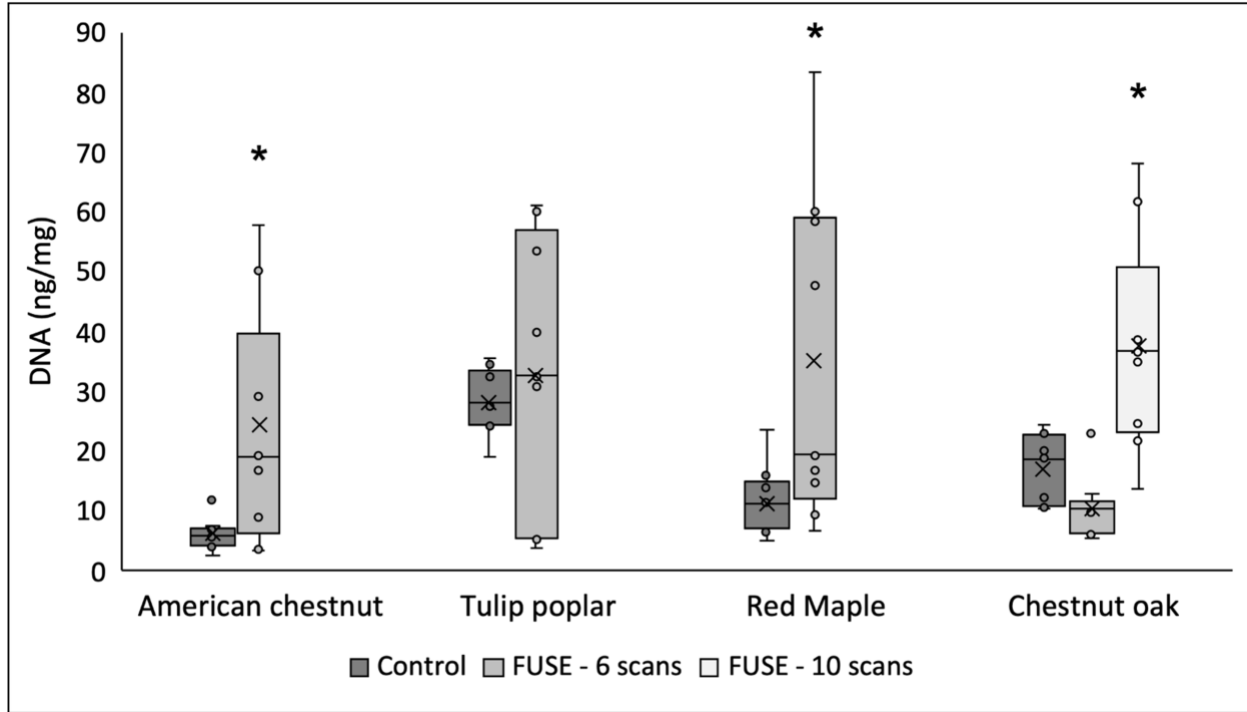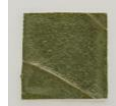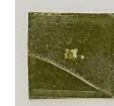
Figure 6: *DNA extraction results show that FUSE releases DNA from leaf tissue. A significant increase in DNA release from American chestnut and red maple samples is observed when processed with 6 FUSE scans compared to controls. DNA release from chestnut oak samples is significantly higher when 10 FUSE scans are used for processing than controls. After 6 FUSE scans, DNA release from tulip poplar samples is comparable to controls. *Indicate significant ($p<0.05$) differences between FUSE and control samples.*
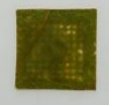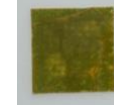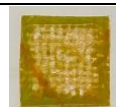
Table 1: *American chestnut tissue breakdown after FUSE processing demonstrates that greater tissue disintegration increases the concentration of DNA release. DNA quantification measurements are reported from Qubit™ Fluorometer measurements, and 260/280 and 260/230 ratios are reported from Nanodrop™ measurements.*

Leaf Species	Description	Data	Sample 1	Sample 2	Sample 3
American Chestnut Leaf 1	Large, thick, dark green	6 scans			
		DNA (ng/mg)	29.48	29.32	50.14
		260/280	1.75	1.66	1.72
		260/230	2.16	1.72	2.01

23

American Chestnut Leaf 2	Large, dry, brown green	6 scans			
		DNA (ng/mg)	16.68	19.30	58.11
		260/280	3.43	4.27	2.04
		260/230	26.65	-4.40	1.72
American Chestnut Leaf 3	Large, dry, brown green	6 scans			
		DNA (ng/mg)	3.31	3.65	8.95
		260/280	2.60	1.64	1.91
		260/230	-0.94	-2.22	-5.77

406
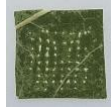
Table 2: *Tulip poplar tissue breakdown after FUSE processing demonstrates that greater tissue disintegration increases the concentration of DNA release. DNA quantification measurements are reported from Qubit™ Fluorometer measurements, and 260/280 and 260/230 ratios are reported from Nanodrop™ measurements.*

Leaf Species	Description	Data	Sample 1	Sample 2	Sample 3
Tulip Poplar Leaf 1	Large, thick, dark green	6 scans			
		DNA (ng/mg)	5.25	30.89	5.65
		260/280	1.53	1.82	1.60
		260/230	2.59	2.12	1.16
Tulip Poplar Leaf 2	Small, wet, yellow green	6 scans			
		DNA (ng/mg)	53.64	60.28	61.32
		260/280	1.83	1.85	1.75
		260/230	1.50	1.88	1.69
Tulip Poplar Leaf 3	Small, wet, yellow green	6 scans			
		DNA (ng/mg)	3.71	32.70	40.06
		260/280	2.09	1.70	1.72
		260/230	-1.06	1.23	1.58

410

24
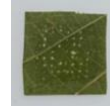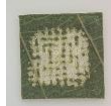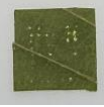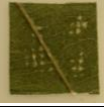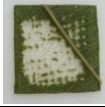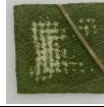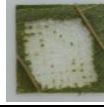
411   **Table 3:** *Red maple tissue breakdown after FUSE processing demonstrates that greater tissue disintegration increases*

412   *the concentration of DNA release. DNA quantification measurements are reported from Qubit^{TM} Fluorometer*

413   *measurements, and 260/280 and 260/230 ratios are reported from Nanodrop^{TM} measurements.*

Leaf Species	Description	Data	Sample 1	Sample 2	Sample 3
Red Maple Leaf 1	Large, thick, dark green	6 scans			
		DNA (ng/mg)	47.84	60.12	19.48
		260/280	1.66	1.68	1.48
		260/230	1.73	1.89	1.15
Red Maple Leaf 2	Small, thick, dark green	6 scans			
		DNA (ng/mg)	58.61	16.85	83.51
		260/280	1.80	1.55	1.77
		260/230	2.09	1.59	1.94
Red Maple Leaf 3	Small, thick, dark green	6 scans			
		DNA (ng/mg)	9.55	14.98	6.96
		260/280	1.66	1.46	1.65
		260/230	-1.14	2.43	5.86

414

415   **Table 4:** *Chestnut oak tissue breakdown after FUSE processing demonstrates that greater tissue disintegration*

416   *increases the concentration of DNA release. DNA quantification measurements are reported from Qubit^{TM}*

417   *Fluorometer measurements, and 260/280 and 260/230 ratios are reported from Nanodrop^{TM} measurements.*

Leaf Species	Description	Data	Sample 1	Sample 2	Sample 3
Chestnut Oak Leaf 1	Large, thick, dark green	6 scans			
		DNA (ng/mg)	10.37	12.90	10.92
		260/280	1.60	1.69	1.64
		260/230	3.63	2.79	5.13
		10 scans			

		DNA (ng/mg)	24.55	21.78	13.69
		260/280	1.66	1.68	1.62
		260/230	1.74	1.86	1.79
Chestnut Oak Leaf 2	Large, thick, dark green	6 scans			
		DNA (ng/mg)	6.46	10.51	6.23
		260/280	2.67	1.84	1.90
		260/230	6.41	-21.12	9.13
		10 scans			
		DNA (ng/mg)	39.91	35.08	61.87
		260/280	1.86	1.87	1.89
		260/230	2.18	2.01	2.07
Chestnut Oak Leaf 3	Large, thick, dark green	6 scans			
		DNA (ng/mg)	5.69	22.90	9.90
		260/280	1.69	1.77	1.75
		260/230	-2.97	2.46	-3.94
		10 scans			
		DNA (ng/mg)	68.18	38.81	36.83
		260/280	1.78	1.77	1.74
		260/230	2.36	3.08	3.42

418

419 The DNA extraction results show that leaf species influenced the DNA yield. Since the leaves

420 chosen represented a range of angiosperm taxonomic diversity, it was expected that differences

421 in physical and chemical properties would affect the quantity of DNA released. The control DNA

422 concentration data was examined to determine the effect of species on DNA release. The

423 American chestnut DNA yield was significantly lower than the average DNA yield from the control

424 samples. The tulip poplar DNA yield was significantly greater than the average DNA yield from

425 the control samples. The American chestnut leaves were the only samples described as brown-

26

426 green, while the tulip poplar leaves were the only samples characterized as yellow-green. These

427 sample characteristics suggest that the American chestnut samples were more mature than the

428 tulip poplar samples at the time of collection [46]. It is common for older leaves to have greater

429 amounts of secondary metabolites, which often cause low yield and poor quality DNA [14].

430 Therefore, it is likely that the age of the sampled leaves influenced inconsistencies in the quantity

431 of the released DNA. As mentioned previously, it is also plausible that species-specific differences

432 influenced the DNA yield. Further investigation into the physical and chemical properties of each

433 leaf species would be needed to confirm this possibility.

434

435 The 260/280 and 260/230 ratios were measured to assess the quality of the DNA extracted with

436 FUSE and conventional methods (Table 5). For American chestnut and chestnut oak, the 260/280

437 ratio was significantly higher for samples processed with six FUSE scans than for control samples.

438 The 260/280 ratio for six FUSE scans was significantly lower than conventional methods for red

439 maple leaves. No discernible trends were observed in 260/230 ratios, with values in expected

440 norms for leaf tissue. However, the 260/30 ratio was significantly higher after ten FUSE scans

441 than controls for chestnut oak leaves. This significant difference is likely the result of increased

442 DNA release due to increased tissue breakdown. Some species processed with FUSE showed high

443 standard error in 260/230 ratios. This result is likely due to incomplete tissue disintegration for

444 some samples within these groups. However, it may also suggest that DNA extraction with FUSE

445 affects the breakdown of compounds that contribute to turbidity in a purified sample.

446 *Table 5: The quality of DNA released by FUSE is comparable to DNA released by conventional methods. FUSE requires*

447 *less processing time than conventional methods and releases greater quantities of DNA. DNA quantification*

448   *measurements are reported from Qubit™ Fluorometer measurements, and 260/280 and 260/230 ratios are reported*

449   *from Nanodrop™ measurements.*

Sample Type	FUSE				Conventional Method			
	Time (mm:ss)	DNA (ng/mg)	260/280	260/230	Time (mm:ss)	DNA (ng/mg)	260/280	260/230
American chestnut	9:00	24.33 ± 6.51	2.34 ± 0.31	2.68 ± 3.51	30:00	6.22 ± 0.87	1.45 ± 0.01	0.52 ± 0.01
Tulip poplar	9:00	32.61 ± 7.82	1.77 ± 0.05	1.41 ± 0.34	30:00	28.37 ± 1.78	1.83 ± 0.01	1.99 ± 0.06
Red maple	9:00	35.32 ± 9.21	1.63 ± 0.04	1.95 ± 0.60	30:00	11.51 ± 1.95	1.85 ± 0.02	2.53 ± 0.19
Chestnut oak 6 scans	9:00	10.65 ± 1.74	1.84 ± 0.11	0.17 ± 3.00	30:00	17.17 ± 1.98	1.52 ± 0.01	0.66 ± 0.02
Chestnut oak 10 scans	15:00	37.85 ± 5.93	1.76 ± 0.03	2.28 ± 0.20	30:00	17.17 ± 1.98	1.52 ± 0.01	0.66 ± 0.02

450

451   The FUSE protocol used in this work involves a non-thermal tissue lysis process that has been

452   shown to reduce the time required for DNA release. The acoustic parameters used in this study,

453   particularly the PRF of 500 Hz, were chosen for this initial feasibility study based on preliminary

454   tissue breakdown experiments. In previous work, Atlantic salmon muscle tissue was processed

455   with FUSE using 10,000 pulses delivered at 25 Hz, which resulted in a total processing time of 6

456   minutes and 40 seconds [20]. In this study, 270,000 pulses were applied at 500 Hz to complete 6

457   FUSE scans, and 450,000 pulses were applied at 500 Hz to complete 10 FUSE scans, resulting in

458   total processing times of 9 and 15 minutes. At higher PRFs, the time efficiency of FUSE was

459   improved without inducing thermal effects. However, further increasing the PRF is likely to result

460   in cavitation shielding effects that lower the effectiveness of each pulse [44, 45]. Future work will

461   be necessary to explore the optimal pulsing parameters for the implementation of higher PRFs.

462   We expect that implementing FUSE at higher PRFs will expand the applicability of FUSE to more

463   robust tissue types and significantly decrease the tissue processing time.

464

465 3.3 DNA amplification

466 American chestnut samples were selected for amplification and sequencing. All FUSE and control

467 samples were amplified with PCR following restriction digestion and adaptor ligation. The

468 samples processed with FUSE and conventional methods amplified successfully, demonstrating

469 that FUSE yielded high-quality DNA from leaf tissue suitable for PCR amplification. A subset of

470 the amplified American chestnut libraries was visualized on a 2100 Bioanalyzer to examine the

471 distribution of DNA fragment sizes for samples processed with FUSE and conventional methods

472 (Figure 7). Most fragments for both the FUSE and control samples were within the expected range

473 of 200-600 bp (Figure S2), suggesting that FUSE does not cause greater DNA fragmentation than

474 conventional extraction methods.
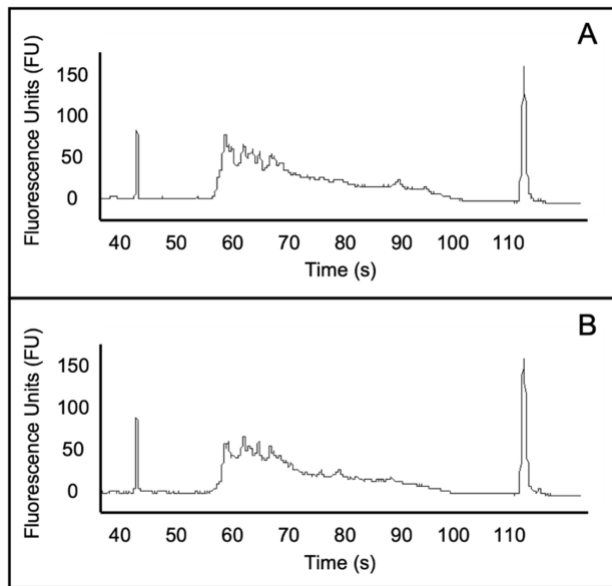

475

476 *Figure 7: The distribution of DNA fragment sizes for an American chestnut sample processed with conventional*

477 *methods (A) is comparable to the DNA fragment size distribution for a sample processed with FUSE (B). This result*

478 *confirms that the integrity of DNA provided by FUSE is suitable for PCR amplification.*

479

480   3.4 Sequencing

481   All American chestnut samples processed with FUSE and conventional methods provided high-

482   quality next-generation sequencing reads (Accession Number: PRJNA837224). Because

483   downstream applications of this technology are expected to be focused on identifying genetic

484   variants from sequence data for population genetics and systematics, we estimated read depth

485   for variable sites, which showed that FUSE samples had a depth comparable to controls. Read

486   depth was moderately correlated between the two extraction methods (Figure S3), and mean

487   depth was not significantly different (25.7 for FUSE and 27.1 for controls; $P=0.155$ based on a

488   Wilcoxon rank-sum test). Among individual FUSE and control samples, read depth was fairly

489   consistent for those processed with FUSE and conventional methods, suggesting that the FUSE

490   protocol yields DNA with quality comparable to conventional methods, and the DNA is suitable

491   for NGS analyses (Figure 8).

492
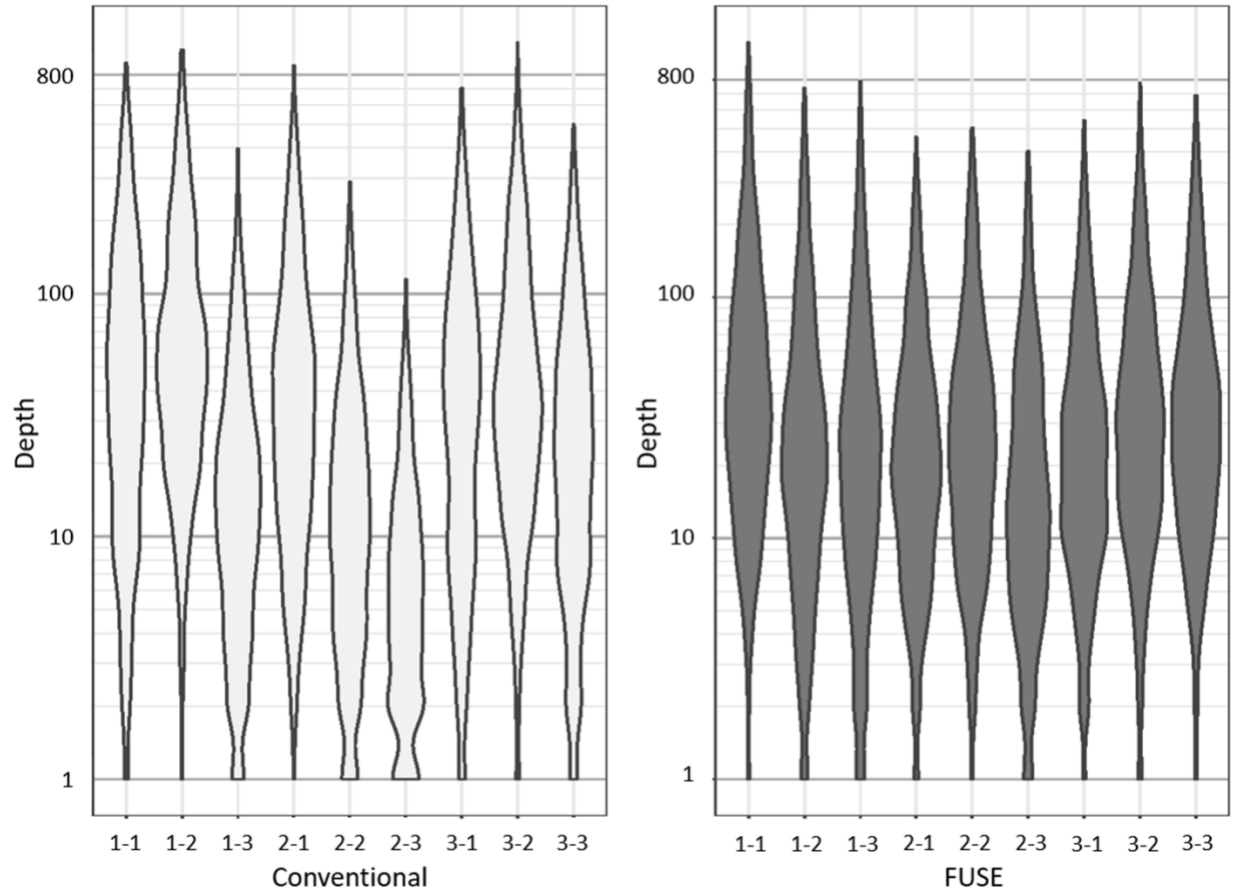
Figure 8: FUSE provides DNA suitable for next-generation sequencing. The uniformity of read depth across conventional and FUSE samples is comparable. The x-axis labeling represents the leaf and sample number, such that 1-2 identifies the read depth for leaf 1, sample 2.

496

4. Conclusion

This study assessed the efficacy of our recently developed FUSE protocol in plant tissues by testing samples from American chestnut, tulip poplar, red maple, and chestnut oak leaves. The success of the FUSE protocol was determined by visualizing the extent of tissue breakdown observed after FUSE sonication, measuring the quantity and quality of the released DNA, and evaluating the suitability of DNA extracts for genetic analyses. PCR amplification and NGS were

503   done to assess the utility of the released DNA in genomic workflows. In accordance with previous

504   work that established the effectiveness of FUSE for releasing DNA from Atlantic salmon muscle

505   tissue [20], the results of this study demonstrate that FUSE can provide high quantities of DNA

506   suitable for amplification and sequencing in less time than conventional plant extraction

507   methods. Additionally, these results suggest that the input sample mass required by FUSE is less

508   than what is necessary for conventional extraction methods, which could be advantageous in

509   future work that aims to develop field-deployable FUSE systems for conservation efforts. Overall,

510   this study shows that the applications of FUSE can be extended to plant tissue, a robust tissue

511   that is more resistant to mechanical breakdown and has a chemical composition that has

512   traditionally made DNA accessibility more challenging [4, 13, 14]. In conjunction with previous

513   findings [20], these results suggest that FUSE could be used as a novel platform for DNA

514   extraction capable of accelerating workflows for a variety of sample types.

515

523

524   **Data Accessibility Statement**

525   All genetic sequences generated in this work are available on Genbank. Next-generation

526   sequencing data can be accessed with the Accession number: PRJNA837224.

527

528   **1. References**

529   [1] Jain, M., Olsen, H.E., Paten, B. & Akeson, M. 2016 The Oxford Nanopore MinION: delivery of

530   nanopore sequencing to the genomics community. *Genome biology* **17**, 1-11.

531   [2] Niemz, A., Ferguson, T.M. & Boyle, D.S. 2011 Point-of-care nucleic acid testing for infectious

532   diseases. *Trends in biotechnology* **29**, 240-250.

533   [3] Dormontt, E.E., Boner, M., Braun, B., Breulmann, G., Degen, B., Espinoza, E., Gardner, S.,

534   Guillery, P., Hermanson, J.C. & Koch, G. 2015 Forensic timber identification: It's time to

535   integrate disciplines to combat illegal logging. *Biological Conservation* **191**, 790-798.

536   [4] Rachmayanti, Y., Leinemann, L., Gailing, O. & Finkeldey, R. 2009 DNA from processed and

537   unprocessed wood: factors influencing the isolation success. *Forensic Science International:*

538   *Genetics* **3**, 185-192.

539   [5] Kersey, P.J. 2019 Plant genome sequences: past, present, future. *Current opinion in plant*

540   *biology* **48**, 1-8.

541   [6] Cornwell, W.K., Pearse, W.D., Dalrymple, R.L. & Zanne, A.E. 2019 What we (don't) know

542   about global plant diversity. *Ecography* **42**, 1819-1831.

543   [7] Halewood, M., Chiurugwi, T., Sackville Hamilton, R., Kurtz, B., Marden, E., Welch, E.,

544   Michiels, F., Mozafari, J., Sabran, M. & Patron, N. 2018 Plant genetic resources for food and

545   agriculture: opportunities and challenges emerging from the science and information

546   technology revolution. *New Phytologist* **217**, 1407-1419.

33

547 [8] Finch, K.N., Jones, F.A. & Cronn, R.C. 2019 Genomic resources for the Neotropical tree genus

548 Cedrela (Meliaceae) and its relatives. *BMC genomics* **20**, 1-17.

549 [9] Finch, K.N., Cronn, R.C., Ayala Richter, M.C., Blanc-Jolivet, C., Correa Guerrero, M.C., De

550 Stefano Beltrán, L., García-Dávila, C.R., Honorio Coronado, E.N., Palacios-Ramos, S. & Paredes-

551 Villanueva, K. 2020 Predicting the geographic origin of Spanish Cedar (Cedrela odorata L.) based

552 on DNA variation. *Conservation Genetics* **21**, 625-639.

553 [10] Group, C.P.W., Hollingsworth, P.M., Forrest, L.L., Spouge, J.L., Hajibabaei, M.,

554 Ratnasingham, S., van der Bank, M., Chase, M.W., Cowan, R.S. & Erickson, D.L. 2009 A DNA

555 barcode for land plants. *Proceedings of the National Academy of Sciences* **106**, 12794-12797.

556 [11] Holliday, J.A., Aitken, S.N., Cooke, J.E., Fady, B., González-Martínez, S.C., Heuertz, M.,

557 Jaramillo-Correa, J.P., Lexer, C., Staton, M. & Whetten, R.W. 2017 Advances in ecological

558 genomics in forest trees and applications to genetic resources conservation and breeding.

559 (Wiley Online Library.

560 [12] Small, R.L., Ryburn, J.A., Cronn, R.C., Seelanan, T. & Wendel, J.F. 1998 The tortoise and the

561 hare: choosing between noncoding plastome and nuclear Adh sequences for phylogeny

562 reconstruction in a recently diverged plant group. *American Journal of Botany* **85**, 1301-1315.

563 [13] Särkinen, T., Staats, M., Richardson, J.E., Cowan, R.S. & Bakker, F.T. 2012 How to open the

564 treasure chest? Optimising DNA extraction from herbarium specimens.

565 [14] Porebski, S., Bailey, L.G. & Baum, B.R. 1997 Modification of a CTAB DNA extraction protocol

566 for plants containing high polysaccharide and polyphenol components. *Plant molecular biology*

567 *reporter* **15**, 8-15.

568   [15] Buser, J.R., Zhang, X., Byrnes, S., Ladd, P., Heiniger, E., Wheeler, M., Bishop, J., Englund, J.,

569   Lutz, B. & Weigl, B. 2016 A disposable chemical heater and dry enzyme preparation for lysis and

570   extraction of DNA and RNA from microorganisms. *Analytical Methods* **8**, 2880-2886.

571   [16] Fredricks, D.N., Smith, C. & Meier, A. 2005 Comparison of six DNA extraction methods for

572   recovery of fungal DNA as assessed by quantitative PCR. *Journal of clinical microbiology* **43**,

573   5122-5128.

574   [17] Yager, P., Domingo, G.J. & Gerdes, J. 2008 Point-of-care diagnostics for global health. *Annu.*

575   *Rev. Biomed. Eng.* **10**, 107-144.

576   [18] Pironon, S., Borrell, J.S., Ondo, I., Douglas, R., Phillips, C., Khoury, C.K., Kantar, M.B., Fumia,

577   N., Soto Gomez, M. & Viruel, J. 2020 Toward unifying global hotspots of wild and domesticated

578   biodiversity. *Plants* **9**, 1128.

579   [19] Wasser, S.K., Brown, L., Mailand, C., Mondol, S., Clark, W., Laurie, C. & Weir, B. 2015

580   Genetic assignment of large seizures of elephant ivory reveals Africa's major poaching hotspots.

581   *Science* **349**, 84-87.

582   [20] Holmes, H.R., Haywood, M., Hutchison, R., Zhang, Q., Edsall, C., Hall, T.L., Baisch, D.,

583   Holliday, J. & Vlaisavljevich, E. 2020 Focused ultrasound extraction (FUSE) for the rapid

584   extraction of DNA from tissue matrices. *Methods in Ecology and Evolution* **11**, 1599-1608.

585   [21] Xu, Z., Hall, T.L., Vlaisavljevich, E. & Lee Jr, F.T. 2021 Histotripsy: the first noninvasive, non-

586   ionizing, non-thermal ablation technique based on ultrasound. *International Journal of*

587   *Hyperthermia* **38**, 561-575.

588   [22] Bader, K.B., Vlaisavljevich, E. & Maxwell, A.D. 2019 For whom the bubble grows: physical

589   principles of bubble nucleation and dynamics in histotripsy ultrasound therapy. *Ultrasound in*

590   *medicine & biology* **45**, 1056-1080.

591   [23] Vlaisavljevich, E., Maxwell, A., Mancia, L., Johnsen, E., Cain, C. & Xu, Z. 2016 Visualizing the

592   histotripsy process: Bubble cloud–cancer cell interactions in a tissue-mimicking environment.

593   *Ultrasound in medicine & biology* **42**, 2466-2477.

594   [24] Mancia, L., Vlaisavljevich, E., Xu, Z. & Johnsen, E. 2017 Predicting tissue susceptibility to

595   mechanical cavitation damage in therapeutic ultrasound. *Ultrasound in medicine & biology* **43**,

596   1421-1440.

597   [25] Kim, Y., Maxwell, A.D., Hall, T.L., Xu, Z., Lin, K.-W. & Cain, C.A. 2014 Rapid prototyping

598   fabrication of focused ultrasound transducers. *IEEE transactions on ultrasonics, ferroelectrics,*

599   *and frequency control* **61**, 1559-1574.

600   [26] Parsons, J.E., Cain, C.A. & Fowlkes, J.B. 2006 Cost-effective assembly of a basic fiber-optic

601   hydrophone for measurement of high-amplitude therapeutic ultrasound fields. *The Journal of*

602   *the Acoustical Society of America* **119**, 1432-1440.

603   [27] Edsall, C., Ham, E., Holmes, H., Hall, T.L. & Vlaisavljevich, E. 2021 Effects of frequency on

604   bubble-cloud behavior and ablation efficiency in intrinsic threshold histotripsy. *Physics in*

605   *Medicine & Biology* **66**, 225009.

606   [28] Edsall, C., Khan, Z.M., Mancia, L., Hall, S., Mustafa, W., Johnsen, E., Klibanov, A.L., Durmaz,

607   Y.Y. & Vlaisavljevich, E. 2021 Bubble cloud behavior and ablation capacity for histotripsy

608   generated from intrinsic or artificial cavitation nuclei. *Ultrasound in Medicine & Biology* **47**, 620-

609   639.

610 [29] Reisman, G., Wang, Y.-C. & Brennen, C.E. 1998 Observations of shock waves in cloud

611 cavitation. *Journal of Fluid Mechanics* **355**, 255-283.

612 [30] Ikeda, T., Yoshizawa, S., Tosaki, M., Allen, J.S., Takagi, S., Ohta, N., Kitamura, T. &

613 Matsumoto, Y. 2006 Cloud cavitation control for lithotripsy using high intensity focused

614 ultrasound. *Ultrasound in medicine & biology* **32**, 1383-1397.

615 [31] Ma, J., Hsiao, C.-T. & Chahine, G.L. 2018 Numerical study of acoustically driven bubble

616 cloud dynamics near a rigid wall. *Ultrasonics sonochemistry* **40**, 944-954.

617 [32] Otsu, N. 1979 A threshold selection method from gray-level histograms. *IEEE transactions*

618 *on systems, man, and cybernetics* **9**, 62-66.

619 [33] Westbrook, J.W., Zhang, Q., Mandal, M.K., Jenkins, E.V., Barth, L.E., Jenkins, J.W.,

620 Grimwood, J., Schmutz, J. & Holliday, J.A. 2020 Optimizing genomic selection for blight

621 resistance in American chestnut backcross populations: A trade-off with American chestnut

622 ancestry implies resistance is polygenic. *Evolutionary applications* **13**, 31-47.

623 [34] Elshire, R.J., Glaubitz, J.C., Sun, Q., Poland, J.A., Kawamoto, K., Buckler, E.S. & Mitchell, S.E.

624 2011 A robust, simple genotyping-by-sequencing (GBS) approach for high diversity species. *PloS*

625 *one* **6**, e19379.

626 [35] Catchen, J., Hohenlohe, P.A., Bassham, S., Amores, A. & Cresko, W.A. 2013 Stacks: an

627 analysis tool set for population genomics. *Molecular ecology* **22**, 3124-3140.

628 [36] Schoch, C.L., Ciufo, S., Domrachev, M., Hotton, C.L., Kannan, S., Khovanskaya, R., Leipe, D.,

629 Mcveigh, R., O'Neill, K. & Robbertse, B. 2020 NCBI Taxonomy: a comprehensive update on

630 curation, resources and tools. *Database* **2020**.

631 [37] McKenna, A., Hanna, M., Banks, E., Sivachenko, A., Cibulskis, K., Kernytsky, A., Garimella,

632 K., Altshuler, D., Gabriel, S. & Daly, M. 2010 The Genome Analysis Toolkit: a MapReduce

633 framework for analyzing next-generation DNA sequencing data. *Genome research* **20**, 1297-

634 1303.

635 [38] Poplin, R., Ruano-Rubio, V., DePristo, M.A., Fennell, T.J., Carneiro, M.O., Van der Auwera,

636 G.A., Kling, D.E., Gauthier, L.D., Levy-Moonshine, A. & Roazen, D. 2018 Scaling accurate genetic

637 variant discovery to tens of thousands of samples. *BioRxiv*, 201178.

638 [39] Mørch, K.A. 2015 Cavitation inception from bubble nuclei. *Interface Focus* **5**, 20150006.

639 [40] Atchley, A.A. & Prosperetti, A. 1989 The crevice model of bubble nucleation. *The Journal of*

640 *the Acoustical Society of America* **86**, 1065-1084.

641 [41] Miller, D.L. 1983 The botanical effects of ultrasound: A review. *Environmental and*

642 *Experimental Botany* **23**, 1-27.

643 [42] Miller, D.L. 1977 The effects of ultrasonic activation of gas bodies in Elodea leaves during

644 continuous and pulsed irradiation at 1 MHz. *Ultrasound in medicine & biology* **3**, 221-240.

645 [43] Xu, Z., Fowlkes, J.B. & Cain, C.A. 2006 A new strategy to enhance cavitational tissue erosion

646 using a high-intensity, initiating sequence. *IEEE transactions on ultrasonics, ferroelectrics, and*

647 *frequency control* **53**, 1412-1424.

648 [44] Pishchalnikov, Y.A., McAteer, J.A., Bailey, M.R., Pishchalnikova, I.V., Williams Jr, J.C. & Evan,

649 A.P. 2006 Acoustic shielding by cavitation bubbles in shock wave lithotripsy (SWL). In *AIP*

650 *Conference Proceedings* (pp. 319-322, American Institute of Physics.

651   [45] Maeda, K., Maxwell, A.D., Colonius, T., Kreider, W. & Bailey, M.R. 2018 Energy shielding by

652   cavitation bubble clouds in burst wave lithotripsy. *The Journal of the Acoustical Society of*

653   *America* **144**, 2952-2961.

654   [46] Goralka, R.J., Schumaker, M.A. & Langenheim, J.H. 1996 Variation in chemical and physical

655   properties during leaf development in California bay tree (Umbellularia californica): Predictions

656   regarding palatability for deer. *Biochemical Systematics and Ecology* **24**, 93-103.

657